20th Australasian Fluid Mechanics Conference
Perth, Australia
5-8 December 2016

Torsional Galloping Marine Current Energy Extraction

B. Stappenbelt and A. D. Johnstone

School of Mechanical, Materials and Mechatronic Engineering
University of Wollongong, New South Wales, 2522, Australia

Abstract

This paper investigated the potential of torsional galloping as an ocean renewable energy mechanism to harvest marine current and tidal stream energy. The torsional galloping phenomenon is a fluid-elastic instability. Steady uniform fluid flow past the structure results in oscillatory rotational motion around a central axis. The use of this mechanism to harvest the energy in fluid flows has received very little attention to date. The present investigation examined the performance of flat plate structures only, covering plate aspect ratios ranging from 0.4 to 1.5. Electrical eddy current damping was applied to the system to simulate the power take-off or energy harvesting from the device. A maximum power extraction efficiency of a modest 5.1% was observed at the lowest aspect ratio trialled. The study also provided an improved understanding of how the response amplitude and frequency are affected by the power take-off damping.

Introduction

The subject of fluid flow-induced vibration (FIV) has long been investigated for its detrimental effects on marine structures (e.g the work by Du and Sun [5], Thorsen et al. [16] and Bokaian and Geoola [4].

Flow-induced oscillations are the vibrations of an object, which occur when an elastic restrained structure is excited by a flow under conditions when the structural damping is not significant enough to decay the motion [17]. These oscillations can be classified into two types, resonance and instability, with each having its own sub-classifications, as shown in Figure 1. It should be noted that the basic types of flow-induced oscillations are not independent, and there may be more than one occurring at any given time [14].

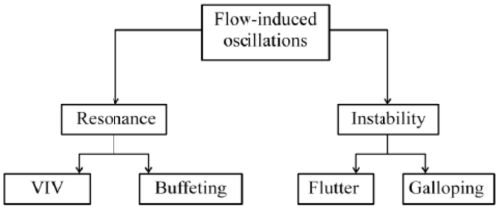

Figure 1. Flow-induced oscillations flow chart (adapted from Fernandes and Armandei [7])

Over the past decade, the marine current and tidal stream energy harvesting potential of flow-induced vibration has been explored. One of the FIV mechanism proposed for this purpose is vortex induced vibrations (VIV). The shedding of vortices from an object in a flow causes the structure to vibrate at one of its natural frequencies. A few groups of researchers have successfully created and implemented devices which are able to harvest the energy for power generation from VIV (e.g. Bernitsas et al. [2], Johnstone and Stappenbelt [11] and Liu et al. [12]).

Also of growing interest in the field of flow-induced vibration energy extraction is the galloping instability of an elastically restrained structure. In the studies by Johnstone and Stappenbelt [10, 11] for example, translational galloping of a cylinder with splitter-plates was employed to extract energy from steady uniform flow. To a far lesser degree, torsional galloping has also been examined recently. The studies by Fernandes and Armandei [7, 8], provided numerical analysis of torsional galloping and experimentation with an associated energy harvesting device.

Galloping can be defined as a hydrodynamic instability; a type of flow induced vibration which causes a structure to oscillate in a sustained manner in a single degree of freedom in either a translating or torsional motion [17]. Translational galloping occurs when the structure undergoes oscillations which may be transverse (perpendicular to fluid flow) [15], longitudinal (parallel to fluid flow), or both [17]. Torsional galloping is defined as the oscillatory motion when the structure is free to rotate on a hinged axis [9]. It can be further defined as either hard galloping, requiring an external influence to start the motion, or soft galloping, which is self-initiating [13].

In their study of low-head hydropower extraction through torsional galloping, Fernandes and Armandei [7] found that oscillatory motions were only produced over a certain range of reduced velocities, having well defined minima and maxima thresholds (see Figure 2). No oscillations were observed below a threshold reduced velocity and static instability, consisting of a constant extreme deflection of the object from its neutral position, provided an upper limit to the galloping motions. Additionally, Fernandes and Armandei [7] noted a fairly constant displacement amplitude and response frequency across this range. Only slight increases in response amplitude was observed with increasing reduced velocity.

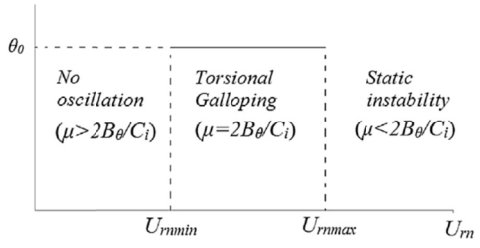

Figure 2. Torsional galloping amplitude predictions through phenomenological modelling (adapted from Fernandes and Armandei [7])

The present paper continues the investigation of the potential of torsional galloping to harvest marine current and tidal stream energy. The fundamental case of flat plate torsional galloping was examined with particular focus on the effect of power take-off (PTO) damping and plate aspect ratios.

Methodology

Steady uniform current conditions were simulated by towing test sections along a 32.5m long 1m×1m cross-section tank. The present investigation examined the torsional galloping performance of flat plate structures only, covering plate aspect ratios (*L/D*) ranging from 0.4 to 1.5. This range is larger than previous investigations (e.g. [7]). The plate neutral position for all experimentation was aligned with the towing direction. Although strictly, this represents a case of hard galloping, minor plate misalignment or perturbations in the flow were sufficient to self-initiate the galloping.

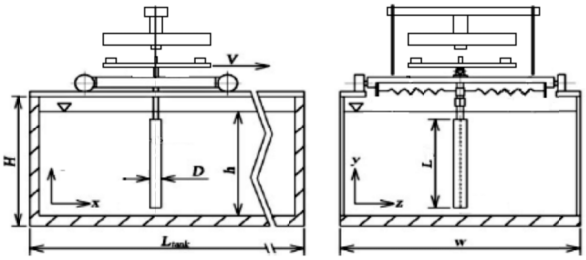

Figure 3. Experimental apparatus sketch

Eddy current damping was applied to the system to simulate the power take-off or energy harvesting from the device. A series of magnets were arranged so that with galloping motions of the test section, they traversed a thick aluminium disc with a set air-gap separating the components (see Figures 3 and 4). Eddy currents are generated in the conductor when there is a relative motion between a magnetic field and the conductor. These eddy currents produce a reactive force which acts in the opposite direction of motion, proportional to velocity in accordance with Lenz's Law. The Eddy current damper therefore behaves as a linear viscous damper [6]. As the distance between the magnet and conductor is increased, the amount of magnetic flux cut by the conductor disc decreases exponentially. An air-gap range of 1 to 7mm was trialled, correlating to a damping ratio range of 0.033 to 0.236. The linear PTO damping distinguishes the present investigation from the prior studies by Fernandes and Armandei [7].

Figure 4. Experimental apparatus mounted on the towing carriage with Eddy current magnetic damper

The torsional stiffness of the rotational system was controlled through a pair of linear springs working on an adjustable lever arm. This allowed variation of the natural frequency of the system. The array of magnets in relative motion to the aluminium disc transferred torque from the shaft through eddy current induction, and provided the power take-off damping. The power output was estimated from measurements of rotary position (and hence velocity) using a non-contact magnetic rotary encoder on the shaft and damping torque using a torque sensor on the aforementioned aluminium disc.

The structural damping ratio in the experimental apparatus was determined to be 2.5% through free decay tests. The Reynolds number range of all experimentation covered a larger range of the subcritical regime than previous torsional galloping energy extraction studies (e.g. [7]). The experimental parameter values and ranges are specified in Table 1.

Parameter	Value
Aspect ratio range (*AR*)	0.4 - 1.5
Plate width (*D*)	0.30 m
Structural damping ratio	0.025
Reduced velocity range (U_r)	1.8 - 3.5
Reynolds number range	$5.77 \times 10^4 - 2.45 \times 10^5$
PTO damping ratio range (ζ)	0.036-0.300

Table 1. Experimental parameter values

Reduced velocity (U_r) values presented in this paper are normalised by the still water natural frequency and plate width (*D*). Only runs where steady state oscillations were observed, after the initial transient response, were included in the analysis.

Results and Discussion

A sample time series of the torsional galloping response measured is presented in Figure 5. This steady state torsional galloping did not occur in all cases trialled. Particularly at the higher aspect ratios and PTO damping, the response motion often transitioned directly from a transient instability (small uneven oscillations around a constant plate deflection angle) to static instability as the reduced velocity increased. The highest aspect ratio plates 1.2 and 1.5 exhibited no signs of steady state torsional galloping under any condition trialled.

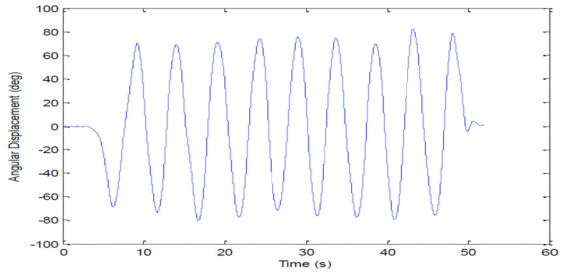

Figure 5. Galloping response time series sample; *AR* = 0.8, ζ = 0.036, *U* = 0.575 m/s)

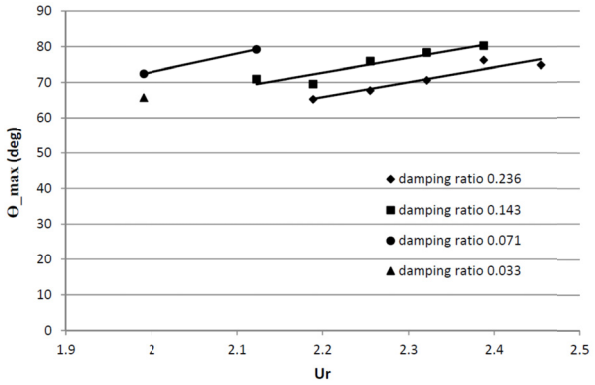

Figure 6. Amplitude response; *AR* = 0.4

The amplitude response plots for the plates with aspect ratios 0.4 and 0.8 are displayed in Figures 6 and 7 respectively. Linear trend lines have been fitted to each PTO damping data set. The torsional galloping response amplitude is observed to increase slightly with reduced velocity. This result is consistent with the conclusions by Fernandes and Armandei [7]. Also discernible

from Figures 6 and 7 is the limited range of reduced velocities over which galloping occurs. No oscillations were observed at reduced velocities below those plotted and static instability was observed at higher reduced velocities. The most significant influence of the PTO damping appears to be to shift the galloping response region to a higher reduced velocity range.

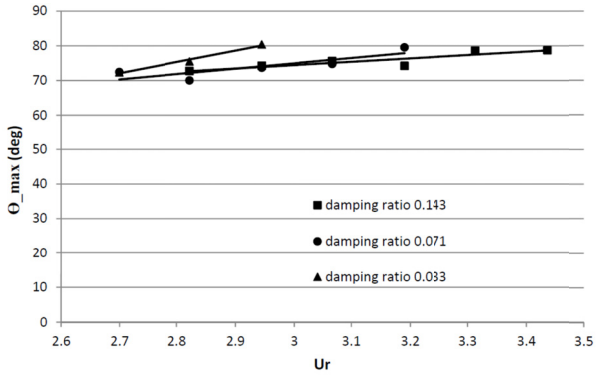

Figure 7. Amplitude response; $AR = 0.8$

As expected, the higher the PTO damping ratio, the lower the galloping oscillation frequency (see Figures 8 and 9). It was also noted that the oscillation frequency increased with increasing aspect ratio.

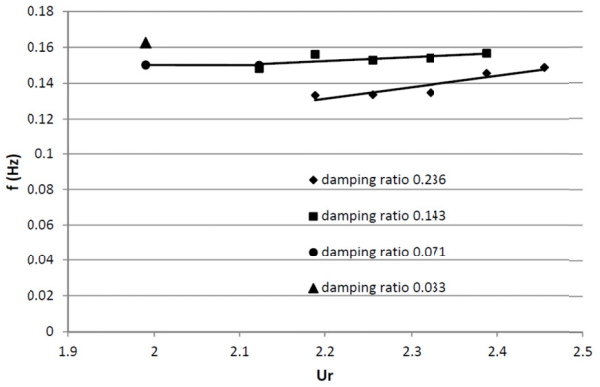

Figure 8. Frequency response; $AR = 0.4$

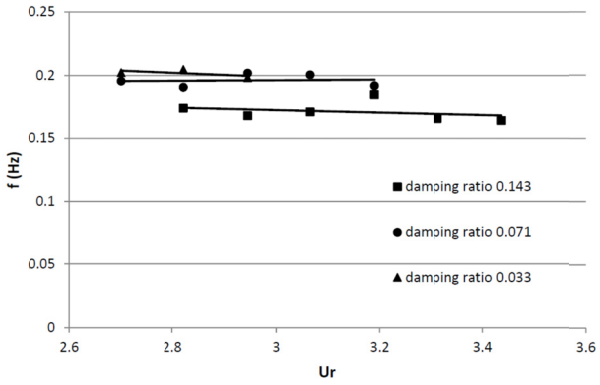

Figure 9. Frequency response; $AR = 0.8$

The galloping reduced velocity range, oscillation amplitude (Θ_{max}), frequency (f) and normalised frequency (f^*) data is summarised in Table 2. Lower frequency oscillations appear to correspond to the lower plate aspect ratios and higher PTO damping. There is insufficient data to draw any meaningful conclusions regarding the effect of PTO damping and plate aspect ratio on the torsional galloping reduced velocity range.

ζ	U_{rnmin}	U_{rrnmax}	Θ_{max} (deg)	f (Hz)	f*
Aspect ratio 0.4					
0.236	2.19	2.45	70.93	0.14	0.28
0.143	2.12	2.39	75.00	0.15	0.31
0.071	1.99	2.12	75.81	0.15	0.30
0.033	1.99	1.99	65.71	0.16	0.32
Aspect ratio 0.6					
0.236	2.49	2.77	67.77	0.13	0.22
0.143	2.49	2.77	78.37	0.17	0.28
0.071	2.36	2.63	70.62	0.17	0.28
0.033	2.36	2.49	74.80	0.18	0.29
Aspect ratio 0.8					
0.143	2.82	3.44	75.69	0.17	0.25
0.071	2.70	3.19	74.10	0.20	0.29
0.033	2.70	2.94	76.09	0.20	0.30
Aspect ratio 0.9					
0.143	3.27	3.51	69.50	0.17	0.24
0.071	3.04	3.39	69.65	0.20	0.28
0.033	2.92	3.27	73.31	0.21	0.29
Aspect ratio 1.0					
0.071	3.14	3.36	65.85	0.18	0.25
0.033	3.14	3.36	71.35	0.20	0.27

Table 2. Summarised experimental results

The power coefficient (C_p) plots for all plate aspect ratios that experienced steady state galloping are presented in Figures 10 to 14. The power coefficient is defined as

$$C_p = \frac{P_{out}}{0.5\rho A U^3} \quad (1)$$

The capture area used in equation 1 is the plate area ($D \times L$). As the actual capture area can be significantly smaller, this does result in the reported power coefficients being conservative.

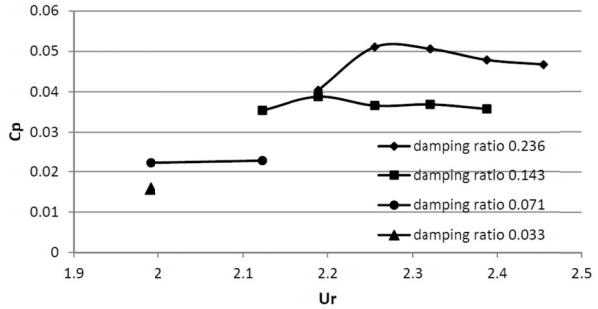

Figure 10. Power coefficient; $AR = 0.4$

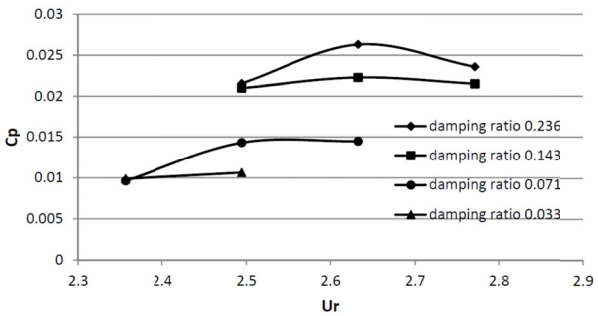

Figure 11. Power coefficient; $AR = 0.6$

The maximum power coefficient observed was 5.1% at an aspect ratio of $AR = 0.4$ and PTO damping of $\zeta = 0.236$. This efficiency is an order of magnitude smaller than Betz's Limit. Although small, the power coefficients achieved are in line with previously reported results for VIV energy extraction using translating [2] and pivoted [11] systems.

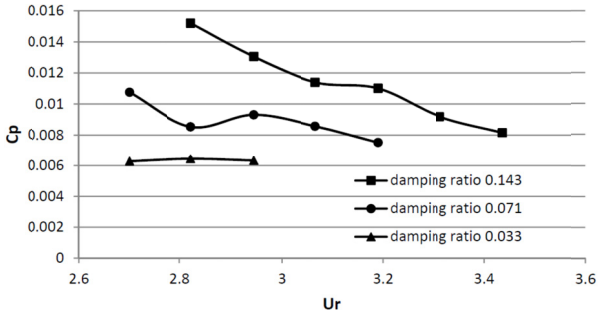

Figure 12. Power coefficient; $AR = 0.8$

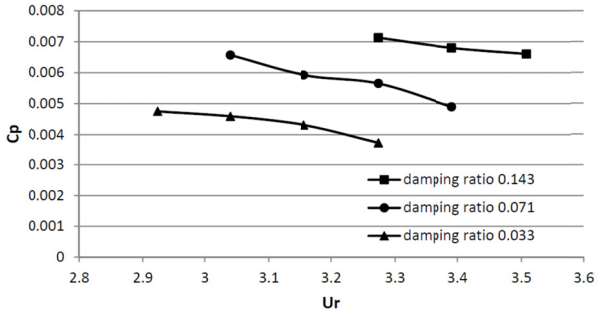

Figure 13. Power coefficient; $AR = 0.9$

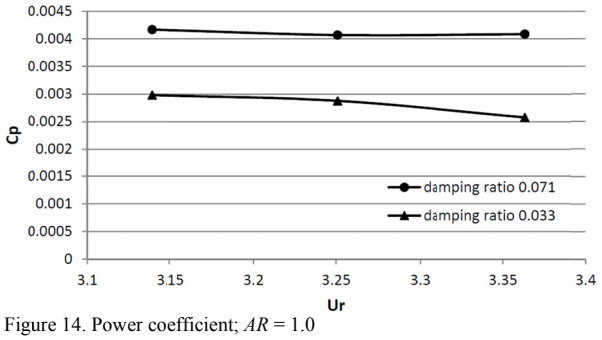

Figure 14. Power coefficient; $AR = 1.0$

Conclusions

The observations made in the current torsional galloping flow-induced vibration energy extraction study are consistent with previous work in this field by Fernandes and Armandei [8]. The response amplitude increases slightly with reduced velocity and the oscillation frequency is relatively unaffected across the reduced velocity range.

The most significant effect of increasing the PTO damping is to shift the galloping response region to a higher reduced velocity range. The smaller the aspect ratio, the better the energy harvesting efficiency with a maximum power coefficient in the present study observed to occur at $AR = 0.4$.

The highest recorded energy harvesting efficiency in the current investigation was 5.1%. As this was observed at the lowest aspect ratio and highest PTO damping trialled, the potential of torsional galloping FIV energy extraction may be better than indicated with this result. Given that similar FIV energy harvesting studies using VIV yield comparable efficiencies, further investigation into the use of torsional galloping would appear to be warranted.

Acknowledgments

The authors gratefully acknowledge the contribution by Mr. Ryan Drury to this study.

References

[1] Assi, G. R. S., Bearman, P. W. & Tognarelli, M. A. On the stability of a free-to-rotate short-tail fairing and a splitter plate as suppressors of vortex-induced vibration. *Ocean Engineering*, 92, 2014, 234-244.

[2] Bernitsas, M. M., Raghavan, K., Ben-Simon, Y. & Garcia, E. M. H. VIVACE (Vortex Induced Vibration Aquatic Clean Energy): A new concept in generation of clean and renewable energy from fluid flow. *Journal of Offshore Mechanics and Arctic Engineering*, 130, 2008.

[3] Bokaian, A. R. & Geoola, F. Hydroelastic instabilities of square cylinders. *Journal of Sound and Vibration*, 92, 1984, 117-141.

[4] Bokaian, A. R. & Geoola, F. Hydroelastic instabilities of square cylinders. *Journal of Sound and Vibration*, 92, 1984, 117-141.

[5] Du, L. & Sun, X. Suppression of vortex-induced vibration using the rotary oscillation of a cylinder. *Physics of Fluids,* 27, 2015.

[6] Ebrahimi, B., Khamesee, M. B. & Golnaraghi, F. Permanent magnet configuration in design of an eddy current damper. *Microsystem Technologies*, 16, 2010, 19-24.

[7] Fernandes, A. C. & Armandei, M. Low-head hydropower extraction based on torsional galloping. *Renewable Energy*, 69, 2014, 447-452.

[8] Fernandes, A. C. & Armandei, M. Marine current energy extraction using torsional galloping based turbine. *Offshore Technology Conference, OTC 2013*, Houston, TX, 2013.

[9] Haaker, T. I. & Van Oudheusden, B. W. One-degree-of-freedom rotational galloping under strong wind conditions. *International Journal of Non-Linear Mechanics*, 32, 1997, 803-814.

[10] Johnstone, A. & Stappenbelt, B. Flow-Induced Vibration Characteristics of Pivoted Cylinders with Splitter-Plates, *Australian Journal of Mechanical Engineering*, Vol. 14, No. 1, 2016, pp.53-63.

[11] Johnstone, A. D. & Stappenbelt, B. Energy Capture Optimisation of 1-Degree-of-Freedom Pivoted Rigid Cylinders Undergoing Flow-Induced Vibration in Cross-Flows. *19th Australasian Fluid Mechanics Conference*. Melbourne, Australia, 2014.

[12] Liu, H., Lin, Y., Shi, M., Li, W., Gu, H., Xu, Q. & Tu, L. A novel hydraulic-mechanical hybrid transmission in tidal current turbines. *Renewable Energy*, 81, 2015, 31-42.

[13] Park, H., Kumar, R. A. & Bernitsas, M. M. Enhancement of flow-induced motion of rigid circular cylinder on springs by localized surface roughness at $3\times10^4 \leq Re \leq 1.\ 2\times10^5$. *Ocean Engineering,* 72, 2013, 403-415.

[14] Robertson, I., Li, L., Sherwin, S. J. & Bearman, P. W. A numerical study of rotational and transverse galloping rectangular bodies. *Journal of Fluids and Structures*, 17, 2003, 681-699.

[15] Stappenbelt, B. Splitter-Plate Wake Stabilisation and Low Aspect Ratio Cylinder Flow-Induced Vibration Mitigation, *International Journal of Offshore and Polar Engineering*, Vol. 20, No. 3, 2010, pp. 190–195.

[16] Thorsen, M. J., Sævik, S. & Larsen, C. M. Fatigue damage from time domain simulation of combined in-line and cross-flow vortex-induced vibrations. *Marine Structures*, 41, 2015, 200-222.

[17] Van Oudheusden, B. W. Rotational one-degree-of-freedom galloping in the presence of viscous and frictional damping. *Journal of Fluids and Structures*, 10, 1996, 673-689.